



# Effects of Inlet-Loss Coefficient on Dynamic Coefficients and Stability of Multistage Pump Annular Seal

Guangkuan Wu<sup>1</sup> · Jianjun Feng<sup>1</sup> · Xingqi Luo<sup>1</sup>

Received: 21 November 2016 / Accepted: 11 July 2018 / Published online: 9 August 2018  
© Shiraz University 2018

## Abstract

In order to explore the influence of inlet-loss coefficient on dynamic coefficients and stability of finite-length annular seal, and then to provide theoretical basis for multistage pump rotor system vibration and stability, the bulk-flow model is taken into account to model the fluid control equations of clearance flow, and perturbation method is applied to calculate the first-order functions and dynamic coefficients. The calculated results are validated by comparing them with reference results, and the minimum and maximum error percentage are 1.4 and 5.6%, respectively. The dynamic coefficients change rule and stability of annular seal under the multifactor-coupled effects are researched in a detailed manner. The numerical results show that the inlet-loss coefficient plays an important role in dynamic coefficients of finite-length annular seal, especially for direct stiffness. All of the dynamic coefficients increase with the increase in inlet-loss coefficient, and the growth trends are the most distinct for large length–diameter ratio, small clearance or high rotating speed. Moreover, reducing the inlet-loss coefficient can improve the stability of annular seal. The research results and conclusions can provide references for the structure design of multistage pump and optimal design of rotor system.

**Keywords** Annular seal · Dynamic coefficients · Inlet-loss coefficient · Perturbation method · Whirl frequency ratio

## 1 Introduction

External excitations, such as the fluid exciting force inside the seal structure between a stator and a rotor or the fluid-film force of bearings, are the key factors that may induce severe vibration and instability in modern rotating machinery (Megerle et al. 2013; Zhou et al. 2014a). Many studies have been carried out to present that the annular seals not only control the leakage, but also obviously affect the dynamic characteristics of rotor system (Hua et al. 2005; Banakh and Nikiforov 2007; Wang et al. 2009; Zhou et al. 2014b). Research on the mechanisms of fluid–solid interaction and the influence of sealing force on rotor system has become the hottest topic for the vibration characteristics of multistage pumps.

The sealing force of annular seal is usually expressed in the form of dynamic coefficients (Kerr 2005; Wang et al.

2016; Jiang et al. 2013). Jenssen and Black first proposed the solving method for direct stiffness, but the calculation error is obvious for large length–diameter ratios because of the greatly simplified control equations (Jenssen 1970; Black 1971, 1974). Based on Hirs' bulk-flow theory, Childs put forward a solving method for finite-length annular seal which expanded the calculation scope of length–diameter ratio (Childs 1983). Nelson and Nguyen developed a new solution to research the effects of eccentricity on rotordynamic coefficients of annular seals by fast Fourier transforms (Nelson and Nguyen 1988a, b). Baskharone et al. established the full-sized scale model of leakage flow channel and compared the calculated results with experimental results (Baskharone et al. 1994). Ha et al. developed a solution procedure to solve the dynamic performances of floating ring seals on the basis of Nelson and Nguyen's method (Ha et al. 2002). Duan et al. applied the bulk-flow model with a steepest descent method to calculate the static and dynamic characteristics of floating ring seals (Duan et al. 2007). With the development of computational fluid dynamics and computer technology, the CFD software has been widely used to calculate the dynamic coefficients and

✉ Guangkuan Wu  
wuguangkuan@xaut.edu.cn

<sup>1</sup> Institute of Water Resources and Hydro-electric Engineering, Xi'an University of Technology, Xi'an 710048, China

explore the internal flow mechanism of annular seals (Lulu et al. 2014; Ha and Choe 2012, 2014; Untaroiu et al. 2013).

Although previous studies paid considerable attention to the dynamic coefficients of annular seals for different geometry structures and operating conditions, few researches have been carried out to discuss the effects of inlet-loss coefficient on dynamic coefficients. Given this, the article studies the multifactor-coupled effects on the dynamic coefficients of finite-length annular seals thoroughly. The bulk-flow model is considered to model the fluid control equations, and the perturbation method is applied to calculate the dynamic coefficients, respectively. The comparison of numerical results with Childs’ calculated results ensures the accuracy of dynamic coefficients. In addition, the influence of inlet-loss coefficient on stability of annular seal is also researched according to whirl frequency ratio. The research results can provide a theoretical basis and references for the study of annular seal dynamic coefficients and structure optimization of multi-stage pump rotor system.

## 2 Annular Seal Model

### 2.1 Dynamic Model

The three typical kinds of seals, including annular seal, interstage seal and interstage pushing seal, in multistage pump are shown in Fig. 1. The fluids in the clearance can generate fluid force on the condition of high rotating speed, large pressure differences and low viscosity liquid. The external fluid force can improve the support stiffness of rotor and greatly affect the dynamic characteristics of rotor system, which is known as Lomakin effect (Lomakin 1958).

Figure 2 shows the dynamic model of annular seal. The pump rotor operates with a rotating speed of  $\omega$ . Meanwhile, the rotor whirls around the geometry center  $O'$  of stator with a whirling speed of  $\Omega$  due to the unbalanced force. The pressure differences on the surface of rotor

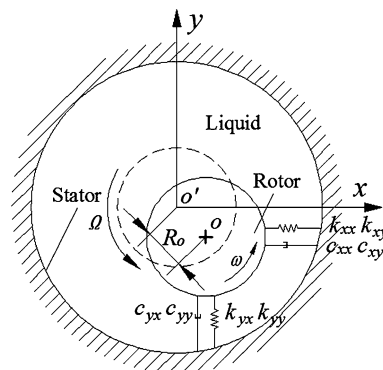


Fig. 2 Dynamic model of annular seal

caused by the eccentric motions in turn produce larger forces in both  $x$  and  $y$  directions. The influence of fluid force on the rotor is described by corresponding dynamic coefficients.

### 2.2 Control Equations with Bulk-Flow Theory

The bulk-flow model has been widely used for the fluid in annular seal, and briefly, the average velocity components replace the variation of fluid velocity components across the clearance in bulk-flow model. Besides, only the shear stress at the shaft and seal stator boundaries is considered for the establishment of control equations. The control equations of finite-length annular seal with bulk-flow theory, i.e., Hirs’ turbulent lubrication equations, can be expressed as (Leqin et al. 2013):

$$\begin{aligned} & \frac{-H^2}{\mu U} \frac{\partial p}{\partial Z} \\ &= \frac{n_0}{2} R_c^{1+m_0} \left\{ u_z (u_\theta^2 + u_z^2)^{\frac{1+m_0}{2}} + u_z [(u_\theta - 1)^2 + u_z^2]^{\frac{1+m_0}{2}} \right\} \\ &+ R_c \left\{ \frac{H}{U} \frac{\partial u_z}{\partial t} + \frac{H u_\theta}{R} \frac{\partial u_z}{\partial \theta} + H u_z \frac{\partial u_z}{\partial Z} \right\} \end{aligned} \quad (1)$$

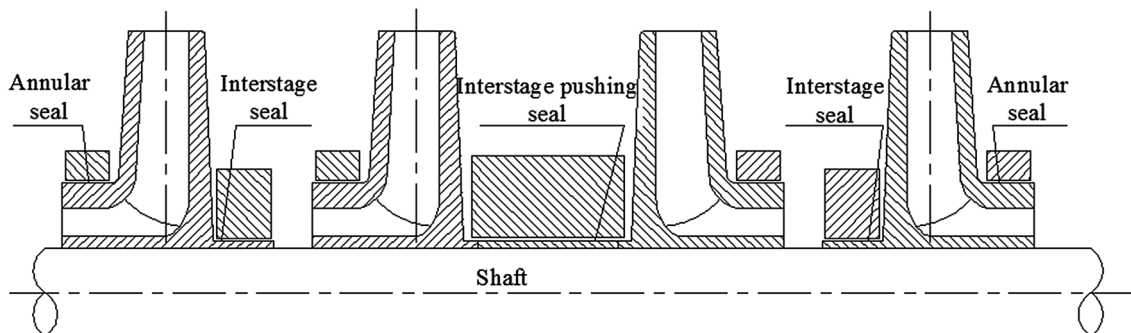


Fig. 1 Schematic of annular seals in multistage pump

$$\begin{aligned} & \frac{-H^2}{\mu U} \frac{1}{R} \frac{\partial p}{\partial \theta} \\ & = \frac{n_0}{2} R_c^{1+m_0} \left\{ u_\theta (u_\theta^2 + u_z^2)^{\frac{1+m_0}{2}} + (u_\theta - 1) \left[ (u_\theta - 1)^2 + u_z^2 \right]^{\frac{1+m_0}{2}} \right\} \\ & + R_c \left\{ \frac{H}{U} \frac{\partial u_\theta}{\partial t} + \frac{H u_\theta}{R} \frac{\partial u_\theta}{\partial \theta} + H u_z \frac{\partial u_\theta}{\partial z} \right\} \end{aligned} \quad (2)$$

$$H \frac{\partial u_z}{\partial z} + \frac{1}{R} \frac{\partial}{\partial \theta} (H u_\theta) + \frac{1}{R \omega} \frac{\partial H}{\partial t} = 0 \quad (3)$$

where  $H$  is seal radial clearance,  $\mu$  is fluid viscosity,  $U$  is linear velocity,  $p$  is fluid pressure,  $m_0$  and  $n_0$  are empirical coefficients,  $R_c$  is circumferential Reynolds number,  $u_z$  is axial velocity,  $u_\theta$  is circumferential velocity and  $t$  is time.

### 3 Solving of Dynamic Coefficients

#### 3.1 Perturbation Method

In order to solve the dynamic coefficients, the equations are expanded in the perturbation variables:

$$\begin{aligned} u_z &= u_{z0} + \varepsilon u_{z1}, & H &= H_0 + \varepsilon H_1 \\ u_\theta &= u_{\theta 0} + \varepsilon u_{\theta 1}, & p &= p_0 + \varepsilon p_1 \end{aligned} \quad (4)$$

where subscript “0” denotes zero order and “1” denotes first order,  $H_0$  is zero-order seal radial clearance,  $\varepsilon$  is dimensionless seal eccentricity ratio and  $u_z$  and  $u_\theta$  are axial velocity and circumferential velocity, respectively.

The zero-order and the first-order perturbation equations can be obtained by substituting Eq. (4) into control Eqs. (1), (2) and (3). Furthermore, the first-order perturbation of pressure, axial velocity and circumferential velocity can be described as the following form after a series of calculation and dimensionless operation (Childs 1983):

$$\frac{d}{dz} \begin{Bmatrix} \bar{u}_{z1} \\ \bar{u}_{\theta 1} \\ \bar{p}_1 \end{Bmatrix} + [A] \begin{Bmatrix} \bar{u}_{z1} \\ \bar{u}_{\theta 1} \\ \bar{p}_1 \end{Bmatrix} = \left( \frac{r_0}{\varepsilon} \right) \begin{Bmatrix} g_1 \\ g_2 \\ g_3 \end{Bmatrix} \quad (5)$$

$$\text{where } [A] = \begin{bmatrix} 0 & -j \left( \frac{L}{R} \right) & 0 \\ -b \sigma B_4 v & \sigma B_3 + j \Gamma T & -j b \left( \frac{L}{R} \right) \\ (\sigma B_1 + j \Gamma T) / b & \sigma B_2 v + j \omega T & 0 \end{bmatrix},$$

$$\begin{Bmatrix} g_1 \\ g_2 \\ g_3 \end{Bmatrix} = \begin{Bmatrix} j b \left[ \Omega T - \omega T \left( \frac{1}{2} + v \right) \right] \\ -\sigma B_5 v \\ -(1 - m_0) \sigma - j \left[ \Omega T - \omega T \left( \frac{1}{2} + v \right) \right] \end{Bmatrix},$$

$\Gamma = \Omega - \omega \left( \frac{1}{2} - v \right)$ ,  $j$  is imaginary number,  $v$  is swirl-circumferential velocity,  $b$ ,  $B_2$ ,  $B_3$ ,  $B_4$  and  $B_5$  are related to geometry parameters and operation conditions and  $\bar{u}_{z1}$ ,  $\bar{u}_{\theta 1}$  and  $\bar{p}_1$  are just the functions of  $z$ .

Solution of Eq. (5) according to the boundary conditions is relatively explicit and the solution of pressure can be expressed as:

$$\bar{p}_1 = \left( \frac{r_0}{\varepsilon} \right) \{ f_c(z) + j f_s(z) \} \quad (6)$$

#### 3.2 Dynamic Coefficients

Solution for the dynamic coefficients can be undertaken when the pressure field solution of Eq. (6) is obtained. The nondimensional dynamic coefficients can be solved under the definition of reaction force and the hypothesis of small disturbance (Childs 1983):

$$\begin{cases} \bar{K} + \bar{c}(\Omega T) - \bar{M}(\Omega T)^2 = \zeta \int_0^1 f_c(z) dz \\ \bar{k} - \bar{C}(\Omega T) = -\zeta \int_0^1 f_s(z) dz \end{cases} \quad (7)$$

where  $\zeta = 2\sigma / (1 + \zeta + 2\sigma)$ ,  $\zeta$  being inlet-loss coefficient.

The generation reason for inlet-loss attributes to the change of flowing space at the high pressure entrance of annular seal. When the fluid flows from the external chamber into the sealing channel, the fluid velocity can significantly increase and the corresponding pressure suddenly decreases. This pressure drop phenomenon caused by the sudden shrink of seal entrance can be described by introducing the inlet-loss coefficient.

The cross-coupled mass coefficient is ignored because the calculated value is too small. It must be noted that the equation cannot be solved on the condition of one specific whirling speed; therefore, at least three different whirling speeds are applied to determine the five dynamic coefficients (Zhai et al. 2015). Equation (7) can be transformed into the following matrix form:

$$\begin{aligned}
 & \begin{bmatrix} 1 & (\Omega T)_1 & -(\Omega T)_1^2 \\ 1 & (\Omega T)_2 & -(\Omega T)_2^2 \\ \vdots & \vdots & \vdots \\ 1 & (\Omega T)_{i-1} & -(\Omega T)_{i-1}^2 \\ 1 & (\Omega T)_i & -(\Omega T)_i^2 \end{bmatrix} \begin{Bmatrix} \bar{K} \\ \bar{c} \\ \bar{M} \end{Bmatrix} \\
 & = \zeta \begin{Bmatrix} \int_0^1 f_{c,1}(z) dz \\ \int_0^1 f_{c,2}(z) dz \\ \vdots \\ \int_0^1 f_{c,i-1}(z) dz \\ \int_0^1 f_{c,i}(z) dz \end{Bmatrix}, \begin{bmatrix} 1 & -(\Omega T)_1 \\ 1 & -(\Omega T)_2 \\ \vdots & \vdots \\ 1 & -(\Omega T)_{i-1} \\ 1 & -(\Omega T)_i \end{bmatrix} \begin{Bmatrix} \bar{k} \\ \bar{c} \end{Bmatrix} \\
 & = -\zeta \begin{Bmatrix} \int_0^1 f_{s,1}(z) dz \\ \int_0^1 f_{s,2}(z) dz \\ \vdots \\ \int_0^1 f_{s,i-1}(z) dz \\ \int_0^1 f_{s,i}(z) dz \end{Bmatrix} \tag{8}
 \end{aligned}$$

Finally, the dynamic coefficients can be obtained from Eq. (8) and further dimensional conversion.

## 4 Results and Analysis

### 4.1 Validation of Calculated Results

The comparison of the calculated results with Childs' calculated results (Childs 1983) when length–diameter ratios are 0.2 and 0.5 is shown in Table 1. It can be seen that the calculated results show good agreement with

**Table 1** Comparison of literature and calculated results

	Dynamic coefficients	$K$ (N/m)	$k$ (N/m)	$C$ (Ns/m)	$c$ (Ns/m)	$M$ (Ns <sup>2</sup> /m)
$L/D = 0.2$	Literature results	1.865e7	4.213e5	2.235e4	1.206e3	3.2
	Calculated results	1.891e7	4.128e6	2.190e4	1.139e3	3.021
	Error percentage (%)	1.4	2.0	2.0	5.6	5.6
$L/D = 0.5$	Literature results	2.208e7	2.570e7	1.362e5	1.751e4	46.73
	Calculated results	2.270e7	2.496e7	1.324e5	1.670e4	44.318
	Error percentage (%)	2.8	2.9	2.8	4.6	5.4

Childs' results. The maximum and minimum error percentage are 5.6 and 1.4%, respectively, and most error percentages are 1–5%. The differences between literature and calculated results are mainly attributed to the calculation error and fitting of dynamic coefficients. The small error illustrates the method proposed by the paper is feasible, and the calculated results fully satisfy the engineering application (Table 2).

The main geometry parameters and operating parameters of annular seal are listed in Table 3.

### 4.2 Effect of Whirl Speed on Dynamic Coefficients

As shown in Eqs. (7, 8), the dynamic coefficients of annular seal can be calculated by multiple whirl speeds. In order to investigate the whirl speed on dynamic coefficients, three typical groups with different whirl speeds are chosen to determine the dynamic coefficients. Here, the rotating speed  $\omega$  is regarded as the reference number, and the three groups with different whirl speeds are (0 ×, 0.25 ×, 0.5 ×, 0.75 ×, 1 ×), (0 ×, 0.5 ×, 1 ×, 1.5 ×, 2 ×) and (1 ×, 1.25 ×, 1.5 ×, 1.75 ×, 2 ×), respectively (Fig. 3).

The calculated results imply that the effect of whirl speed on damping are more obvious compared with the effect on stiffness, and it can be seen that the maximum error for damping is 1.537%, while it is 0.431% for stiffness. Besides, the stiffness and direct damping increase when the whirl speeds change from group one to group three; on the contrary, the cross-coupled damping decreases with the change of whirl speeds. Overall, the whirl speed has a limited effect on dynamic coefficients in comparison with the effects of sealing parameters. In fact, the second group of whirl speeds is closer to the real operating condition for multistage pump because of the wide and reasonable whirl range.

**Table 2** Specified values for bulk-flow model

	$b$	$B_1$	$B_2$	$B_3$	$B_4$	$B_5$
$L/D = 0.2$	1.5297	1.6776	0.2546	1.0724	0.2036	1.3405
$L/D = 0.5$	1.0051	1.6012	0.4475	1.1488	0.6895	1.4360

**Table 3** Main parameters and values

Parameters	$H_0$ (mm)	$\rho$ (kg/m <sup>3</sup> )	$R$ (m)	$\mu$ (Pa s)	$\omega$ (r/min)	$m_0$	$n_0$
Values	0.2	1000	0.075	0.0013	3000	- 0.25	0.079

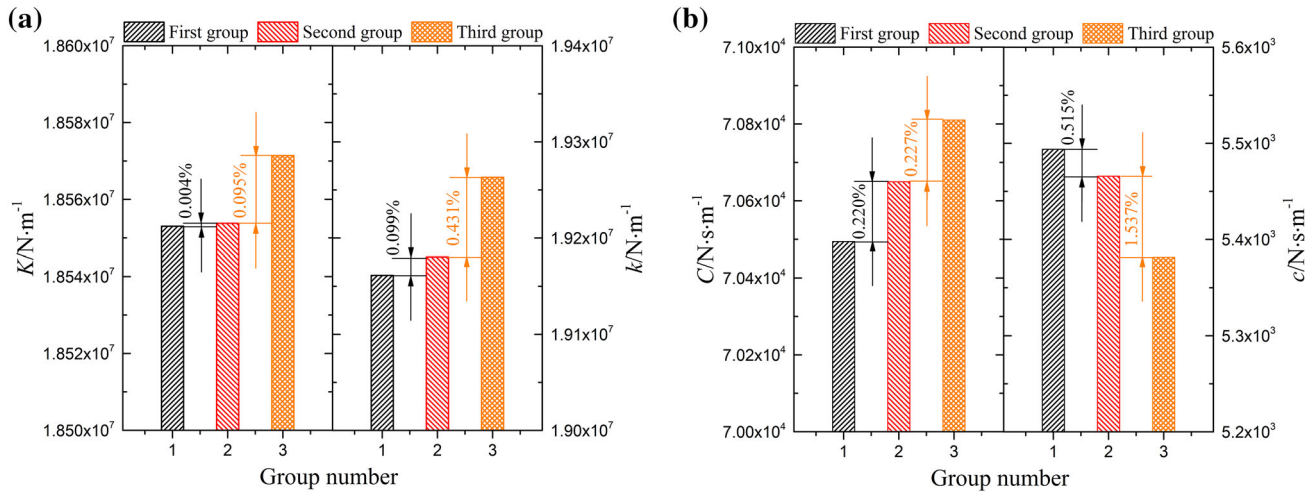


**Fig. 3** Dynamic coefficients versus whirl speed

### 4.3 Effect of $\xi$ on Dynamic Coefficients for Different $L/D$

Figure 4 provides dynamic coefficients change versus the inlet-loss coefficient when  $L/D$  ratio changes from 0.2 to 1. It is shown in Fig. 4a that the increments for direct stiffness when  $L/D$  ratio is 0.2 are smaller than those of large  $L/D$  ratios, which illustrates that the effect of inlet-loss coefficient on the direct stiffness for small  $L/D$  ratio can be neglected. When  $L/D$  ratio is larger than 0.2, the direct stiffness increases with the increase in inlet-loss coefficient on the condition of fixed  $L/D$  ratio. The calculated results imply that the inlet-loss coefficient plays an important role in direct stiffness. In addition, the direct stiffness firstly increases and then decreases as  $L/D$  ratio increases from 0.2 to 1. The reason for the above phenomenon is that when  $L/D$  ratio is small, the axial gradient of pressure is larger than the circumferential gradient of pressure, the pressure drop decreases rapidly, which leads to the small sealing force and direct stiffness. With the increase in  $L/D$  ratio, the sealing force and direct stiffness increase gradually. When  $L/D$  ratio is more than a fixed value, the effect of circumferential gradient of pressure on the sealing force and direct stiffness become more important than that of axial gradient of pressure, and the direct stiffness decreases. From Fig. 4b–d, it can be seen that the cross-coupled stiffness, direct damping and cross-coupled damping increase as inlet-loss coefficient increases and the growth trend is more obvious for high  $L/D$  ratio.

Figure 5 shows the pressure gradient contour in annular seal for different  $\xi$  and  $L/D$ . The pressure presents linear

characteristic with the increase in  $z/L$  ratio. At the same axial position, the pressure decreases as inlet-loss coefficient increases from 0 to 1, while it increases as  $L/D$  ratio increases from 0.1 to 1. It must be noted that the pressure rapidly decreases at the entrance when  $L/D$  ratio is small, which means that the significant reduction in  $L/D$  ratio can seriously weaken the sealing performance of annular seal.

### 4.4 Effect of $\xi$ on Dynamic Coefficients for Different $H_0$

Figure 6 shows dynamic coefficients change versus the inlet-loss coefficient when  $H_0$  increases from 0.1 to 0.3 mm. According to the calculated results shown in Fig. 6a, the direct stiffness increases with the increase in inlet-loss coefficient when the clearance is fixed. Besides, it presents a nonlinear growth trend when the clearance is larger than 0.15 mm, which indicates that the effect of inlet-loss coefficient on direct stiffness weakens in the case of large clearance. It also must be mentioned that the difference of direct stiffness is the smallest regardless of inlet-loss coefficient and increases while inlet-loss coefficient increases to 1 for different clearances. This is because larger radial clearance weakens the Lomakin effect, and the sealing force decreases while the radial clearance increases. The simulated results are consistent with the calculated results of Wang et al. (2016) and Jiang et al. (2013). The changing trends of cross-coupled stiffness, direct damping and cross-coupled damping, shown in Fig. 6b–d, are similar to those obtained for different inlet-loss coefficients

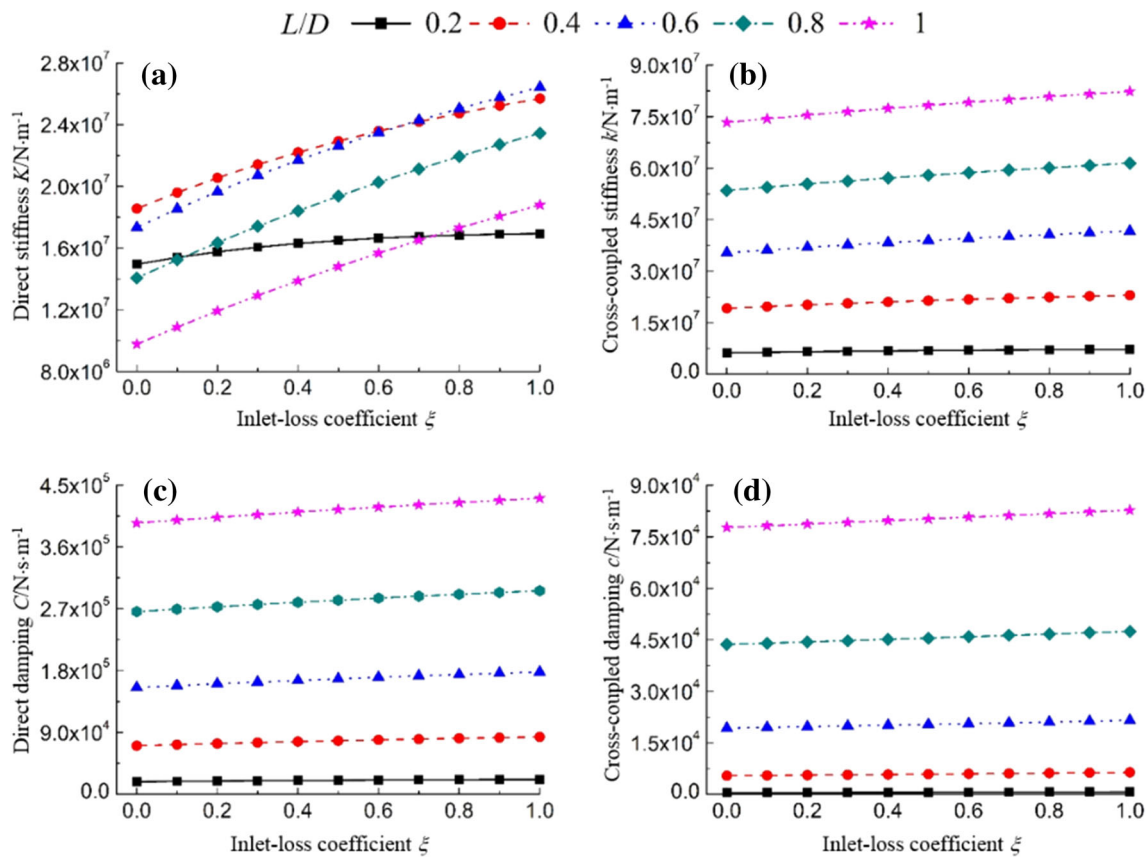


Fig. 4 Dynamic coefficients versus  $\xi$  with different  $L/D$

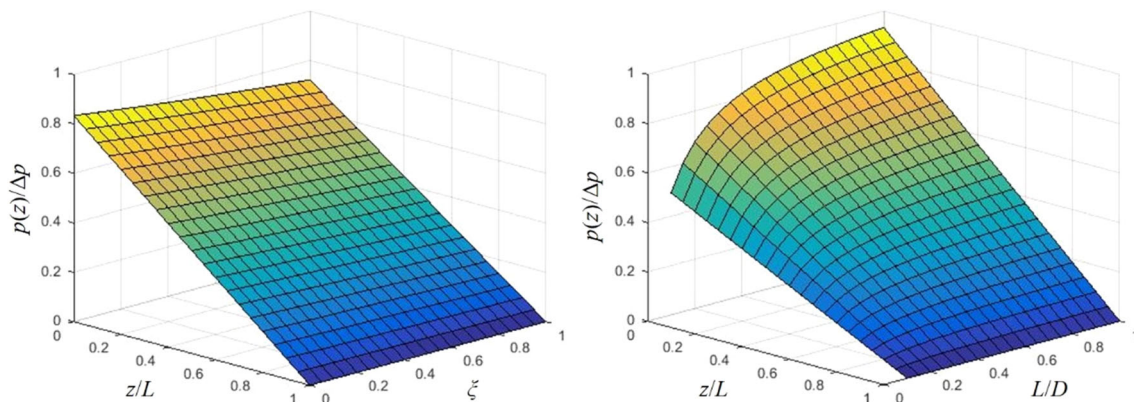


Fig. 5 Pressure gradient contour for different  $\xi$  and  $L/D$

and  $L/D$  ratios. Totally, reducing the clearance is beneficial for the increase in dynamic coefficients.

#### 4.5 Effect of $\xi$ on Dynamic Coefficients for Different $\omega$

The effect of inlet-loss coefficient on dynamic coefficients when the rotating speed changes from 1000 to 5000 r/min is shown in Fig. 7. As shown in Fig. 7a–c, the difference in

dynamic coefficients is not obvious and the changing curves nearly overlap for different rotating speeds, especially for direct stiffness. Though the higher rotating speed can enhance the fluids turbulence level in annular seal and improve the circumferential velocity, the inlet-loss coefficient directly influences the inlet pressure of annular seal on condition of fixed pressure drop, which is known to play an important role in sealing force. The calculated results mean that the effects of inlet-loss coefficient on direct

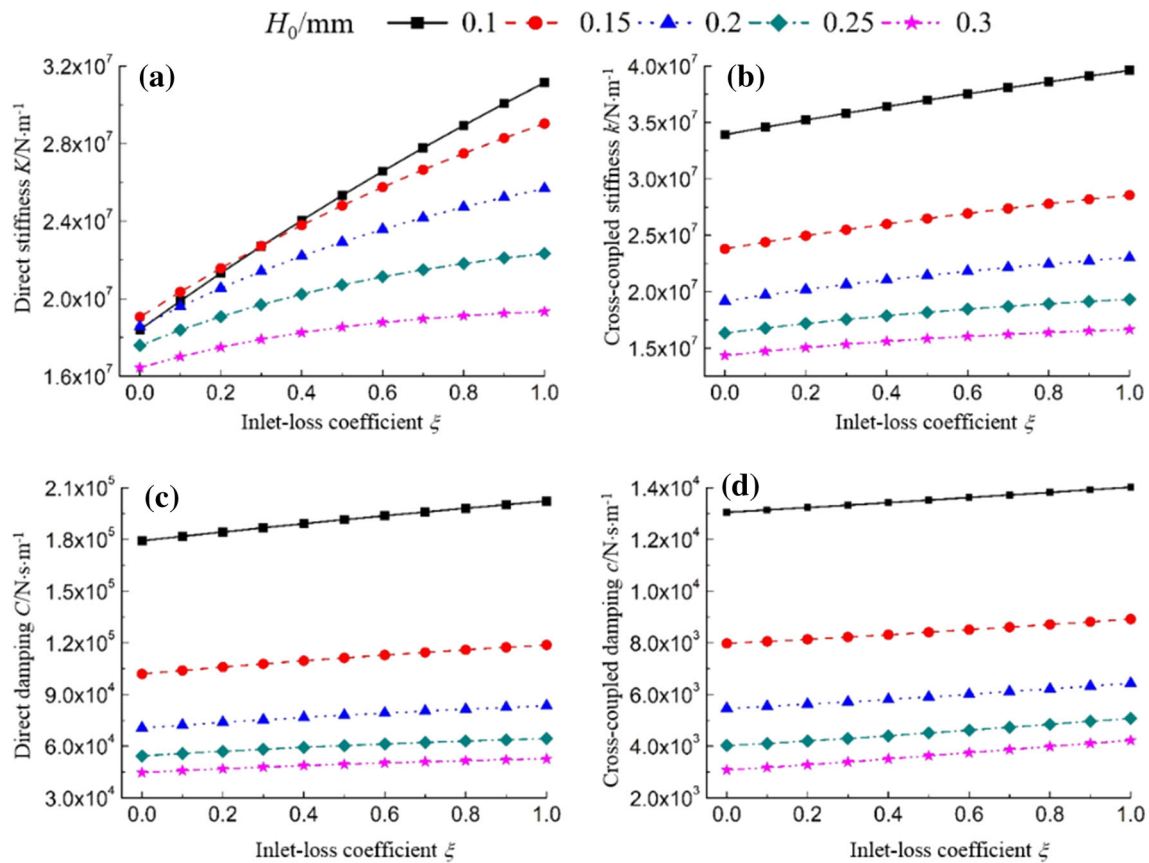


Fig. 6 Dynamic coefficients versus  $\xi$  with different  $H_0$

stiffness and direct damping are greater than rotating speed. Besides, these two dynamic coefficients also present weak nonlinear growth trend. From Fig. 7b, d, it can be seen that the cross-coupled stiffness and damping increase as inlet-loss coefficient increases. However, the increments of these two dynamic coefficients for different rotating speeds on the condition of fixed inlet-loss coefficient are more average than those for different  $L/D$  ratios and clearances.

#### 4.6 Effect of $\xi$ on Stability

The whirl frequency ratio is usually applied to assess the stability of annular seal, which can be expressed as (Leqin et al. 2013):

$$f_w = \frac{k}{\omega C} \tag{9}$$

Actually, the stability of annular seal decreases with the increase in whirl frequency ratio. The relationship between whirl frequency ratio and inlet-loss coefficient is shown in Fig. 8. Note that the minimum value of whirl frequency ratio is 0.864 ignoring the inlet-loss coefficient, while the maximum value is 0.878. The whirl frequency ratio increases as the inlet-loss coefficient increases, but

increments grow more and more slowly. That is to say, smaller inlet-loss coefficient can improve the stability of annular seal.

### 5 Conclusions

Based on the bulk-flow model and perturbation method, the effects of inlet-loss coefficient on the dynamic coefficients for different length–diameter ratios, clearances and rotating speeds are investigated. The whirl frequency ratio is also applied to study the effect of inlet-loss coefficient on the stability of annular seal. The contribution of the current work can be described with the following highlights:

1. The inlet-loss coefficient plays an important role in dynamic coefficients of annular seal, especially for direct stiffness, which means that the influence of inlet-loss coefficient must be considered in the calculation of dynamic coefficients of annular seal and further multistage pump rotor system.
2. The direct stiffness presents approximate linear growth trend with the increase in inlet-loss coefficient. In addition, the direct stiffness firstly increases and then decreases as  $L/D$  ratio increases from 0.2 to 1, while it

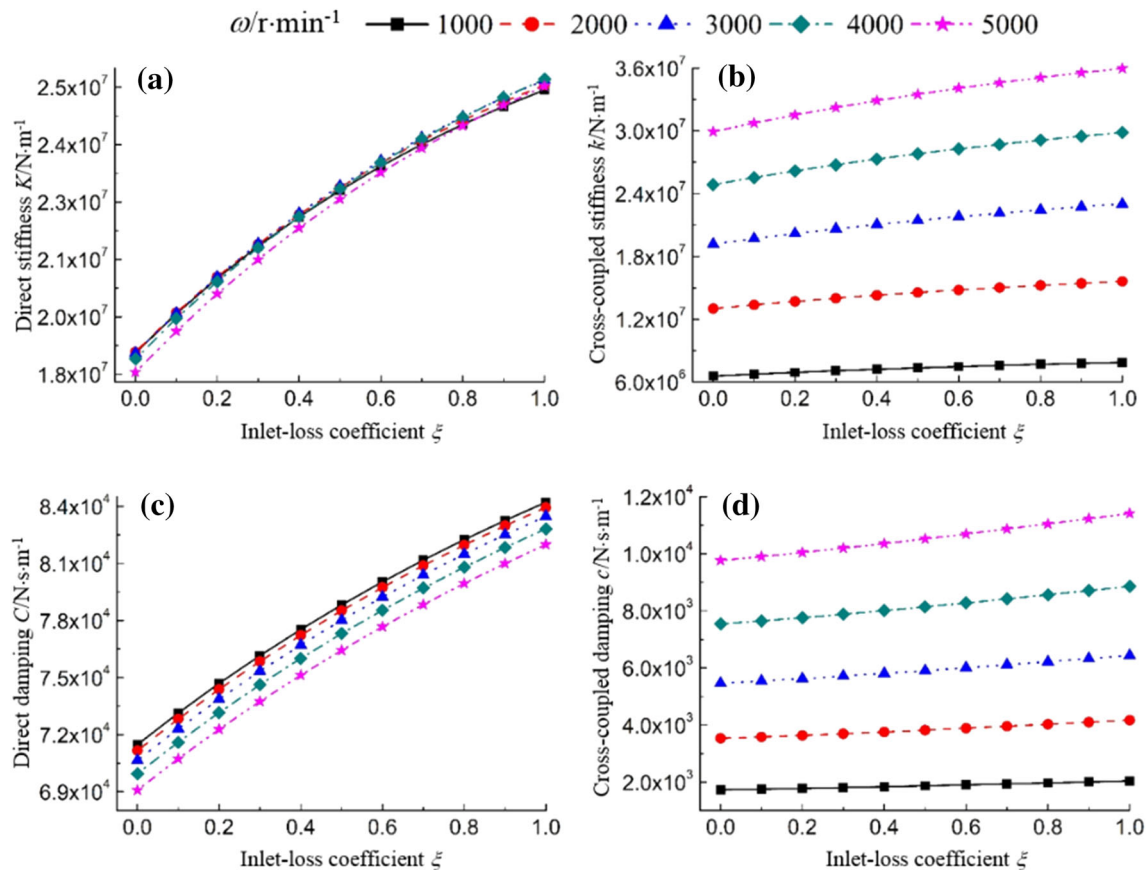


Fig. 7 Dynamic coefficients versus  $\xi$  with different  $\omega$

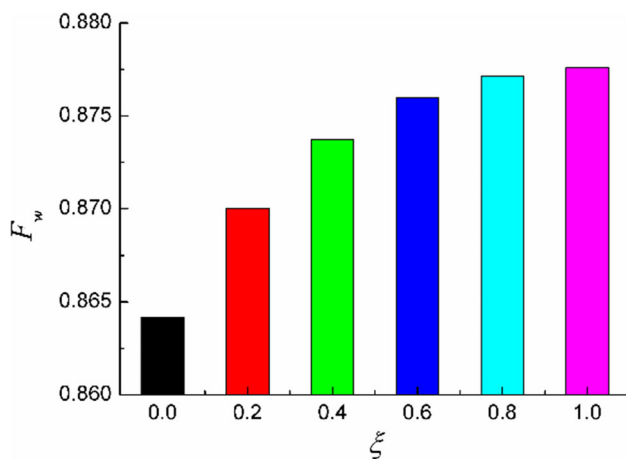


Fig. 8 Whirl frequency ratio versus  $\xi$

decreases as clearance increases from 0.1 to 0.3 mm for fixed inlet-loss coefficient.

- The cross-coupled stiffness, direct damping and cross-coupled damping increase as inlet-loss coefficient increases, and the growth trends are more obvious when length–diameter ratio is 1, zero-order seal radial clearance is 0.1 mm or rotating speed is 5000 r/min,

which demonstrates that the effect of inlet-loss coefficient on these three dynamic coefficients is more evident for large length–diameter ratio, small clearance or high rotating speed.

- The stability of annular seal increases as the inlet-loss coefficient decreases, i.e., small inlet-loss coefficient is in favor of the stability of annular seal.

**Acknowledgement** We acknowledge the financial support from the National Natural Science Foundation of China (No. 51479167) and (No. 51339005).

## References

- Banakh L, Nikiforov A (2007) Vibroimpact regimes and stability of system “rotor—sealing ring”. *J Sound Vib* 308(3):785–793
- Baskharone EA, Daniel AS, Hensel SJ (1994) Rotordynamic effects of the shroud-to-housing leakage flow in centrifugal pumps. *J Fluids Eng* 116(3):558–563
- Black HF (1971) Effects of high-pressure ring seals on pump rotor vibrations. *Fluid Eng Div* 184(3):92–100
- Black HF (1974) Calculation of forced whirling and stability of pump rotor vibrations. *J Manuf Sci Eng* 96(3):1076–1081
- Childs DW (1983) Finite-length solutions for rotordynamic coefficients of turbulent annular seals. *J Tribol* 105(3):437–444



- Duan W, Chu F, Kim CH et al (2007) A bulk-flow analysis of static and dynamic characteristics of floating ring seals. *Tribol Int* 40(3):470–478
- Ha TW, Choe BS (2012) Numerical simulation of rotordynamic coefficients for eccentric annular-type-plain-pump seal using CFD analysis. *J Mech Sci Technol* 26(4):1043–1048
- Ha TW, Choe BS (2014) Numerical prediction of rotordynamic coefficients for an annular-type plain-gas seal using 3D CFD analysis. *J Mech Sci Technol* 28(2):505–511
- Ha TW, Lee YB, Kim CH (2002) Leakage and rotordynamic analysis of a high pressure floating ring seal in the turbo pump unit of a liquid rocket engine. *Tribol Int* 35(3):153–161
- Hua J, Swaddiwudhipong S, Liu ZS et al (2005) Numerical analysis of nonlinear rotor–seal system. *J Sound Vib* 283(3):525–542
- Jenssen DN (1970) Dynamics of rotors systems embodying high pressure ring seals. Heriot-Watt Univ, Edinburgh
- Jiang Q, Zhai L, Wang L et al (2013) Fluid–structure interaction analysis of annular seals and rotor systems in multi-stage pumps. *J Mech Sci Technol* 27(7):1893–1902
- Kerr BG (2005) Experimental and theoretical rotordynamic coefficients and leakage of straight smooth annular gas seals. Texas A&M University, College Station
- Leqin W, Wenjie Z, Guikun X et al (2013) Dynamic coefficients of small cone-shaped annular seal rotor. *J Drain Irrig Mach Eng* 31(6):517–522
- Lomakin AA (1958) Calculating of critical speed and securing of dynamic stability of high pressure pumps with reference to forces arising in seal gaps. *Energomashinostroenic* 4(1):1158–1162
- Lulu Z, Chaohua G, Daqing Q et al (2014) Studies of exit pressure recovery coefficient and its effects on dynamic characteristics of annular water seals. *J Vibroeng* 16(5):2406–2417
- Megerle B, Rice TS, McBean I et al (2013) Numerical and experimental investigation of the aerodynamic excitation of a model low-pressure steam turbine stage operating under low volume flow. *J Eng Gas Turbines Power* 135(1):012602
- Nelson CC, Nguyen DT (1988a) Analysis of eccentric annular incompressible seals: part 1—a new solution using fast Fourier transforms for determining hydrodynamic force. *J Tribol* 110(2):354–359
- Nelson CC, Nguyen DT (1988b) Analysis of eccentric annular incompressible seals: part 2—effects of eccentricity on rotordynamic coefficients. *J Tribol* 110(2):361–366
- Untaroiu A, Hayrapetian V, Untaroiu CD et al (2013) On the dynamic properties of pump liquid seals. *J Fluids Eng* 135(5):051104
- Wang WZ, Liu YZ, Meng G et al (2009) Nonlinear analysis of orbital motion of a rotor subject to leakage air flow through an interlocking seal. *J Fluids Struct* 25(5):751–765
- Wang L, Zhou W, Wei X et al (2016) A coupling vibration model of multi-stage pump rotor system based on FEM. *Mechanics* 22(1):31–37
- Zhai L, Wu G, Wei X et al (2015) Theoretical and experimental analysis for leakage rate and dynamic characteristics of herringbone-grooved liquid seals. *Proc Inst Mech Eng Part J J Eng Tribol* 229(7):849–860
- Zhou W, Wei X, Wei X et al (2014a) Numerical analysis of a nonlinear double disc rotor–seal system. *J Zhejiang Univ Sci A* 15(1):39–52
- Zhou W, Wei X, Zhai L et al (2014b) Nonlinear characteristics and stability optimization of rotor–seal–bearing system. *J Vibroeng* 16(2):818–831